Bull. Chem. Soc. Jpn., 69, 3047—3057 (1996)

A Theoretical Study on the Oxidative Addition of a Si–H σ-Bond to [MCl(CO)(PH$_3$)$_2$] (M=Rh or Ir). Similarities to and Differences from [M′(PH$_3$)$_2$] (M′=Pd or Pt) and [RhCl(PH$_3$)$_2$]

Shigeyoshi Sakaki,* Yuka Ujino, and Manabu Sugimoto

Department of Applied Chemistry and Biochemistry, Faculty of Engineering, Kumamoto University,
Kurokami, Kumamoto 860

(Received April 22, 1996)

The Si–H Oxidative Addition to [MCl(CO) (PH$_3$)$_2$] (M = Rh or Ir) was theoretically investigated with ab initio MO/MP2—MP4, SD-CI, and CCD (coupled cluster with double substitutions) methods. This reaction proceeds with a somewhat high activation energy (E_a) and a moderate exothermicity (E_{exo}); when the oxidative addition occurs in the Cl–M–CO plane, $E_a = 19$ kcal mol^{-1} for Rh and 13 kcal mol^{-1} for Ir, and $E_{exo} = 0.4$ kcal mol^{-1} for Rh and 17.4 kcal mol^{-1} for M = Ir. This result is in significant contrast to [M′(PH$_3$)$_2$] (M′ = Pd or Pt) and [RhCl (PH$_3$)$_2$] : the Si–H oxidative addition occurs with a very small barrier for [M′(PH$_3$)$_2$], but a zero barrier and significantly high exothermicity for [RhCl(PH$_3$)$_2$]. The low reactivity of [MCl(CO)(PH$_3$)$_2$] is interpreted in terms of the low energy level of the d orbital, a considerable weakening of the M–Cl and M–CO bonds, and an exchange repulsion between SiH$_4$ and the M d orbital in [MCl(CO)(PH$_3$)$_2$]. The above results indicate that Vaska-type complexes are less favorable for an oxidative addition reaction than [M′(PH$_3$)$_2$] and [RhCl(PH$_3$)$_2$], and that they cannot be used for a catalytic reaction including an oxidative addition which requires a high activation energy.

Transition-metal catalyzed hydrosilylation is one of the important catalytic reactions.[1)] This catalytic cycle involves an oxidative addition of the Si–H σ-bond to the transition-metal complex, an insertion reaction of alkene or alkyne into the M–H or M–SiR$_3$ bond, and a Si–C or C–H reductive elimination as the key elementary processes.[1)] Thus, a transition-metal catalyst that is efficient for hydrosilylation should have a high reactivity for the oxidative addition of a Si–H σ-bond. In this regard, we need detailed knowledge concerning the factors which determine the ease of Si–H oxidative addition in order to realize new developments of transition-metal catalyzed hydrosilylation. However, little is known on how much the Si–H oxidative addition is influenced by such factors as the kind of metal, the oxidation state of the metal, the d electron number, and a co-existing ligand. Although theoretical investigations are expected to provide such detailed knowledge, only a few have actually been carried out on a Si–H oxidative addition to [M′(PH$_3$)$_2$] (M′ = Pt or Pd) and [RhCl(PH$_3$)$_2$] (Eq. 1),[2,3)] whereas many theoretical

$$\mathrm{ML}_n + \mathrm{H{-}SiH_3} \longrightarrow cis\text{-}[\mathrm{MH(SiH_3)L}_n] \qquad (1)$$

studies have been performed on the oxidative additions of H–H,[4—11)] C–H,[2a,2b,3,7c,8b,9,10b,10c,13,14)] and C–C bonds.[2b,7c,8b,12,13a,15)]

In this work, a Si–H oxidative addition to Vaska-type complexes (Eq. 2) is theoretically investigated with ab initio MO/MP2—MP4, SD-CI, and CCD (coupled cluster with double substitutions) methods. We selected this reaction for the following reasons: (i) [RhCl(CO)(PH$_3$)$_2$] has been used as a catalyst for hydrosilylation,[1a)] and several interesting experimental results have been reported on the Si–H oxidative addition to the Vaska complex and similar complexes.[16—19)] (ii) Although the oxidative addition to [M′(PH$_3$)$_2$] has been well investigated,[2,5,6a,8)] the oxidative addition to Vaska-type

$$trans\text{-}[\mathrm{MCl(CO)(PH_3)_2}]+\mathrm{H{-}SiH_3} \longrightarrow [\mathrm{MH(SiH_3)Cl(CO)(PH_3)_2}] \quad (\mathrm{M{=}Rh\ or\ Ir}) \qquad (2)$$

complexes has not been theoretically investigated, except for some pioneering studies,[11)] in which ab initio MO calculations were carried out on the H–H oxidative addition to [IrCl(CO)(PH$_3$)$_2$]; also, the discussion was mainly presented concerning the reason that the oxidative addition occurs on the Cl–Ir–(CO) plane. (iii) Although a comparison between Vaska-type complexes and [M′(PH$_3$)$_2$] is expected to provide useful information, such a comparison has not yet been made. Through this theoretical study, we hope (a) to obtain a detailed understanding of the Si–H oxidative addition to Vaska-type complexes, (b) to elucidate the differences between Rh and Ir, (c) to compare the reactivity between Vaska-type complexes, [M′(PH$_3$)$_2$], and coordinatively unsaturated [RhCl(PH$_3$)$_2$], and (d) to clarify the characteristic features which Vaska-type complexes exhibit in oxidative addition. It is our intention to show clearly that the coordination of CO greatly disfavors an oxidative addition.

Computational Details

All of the geometries including the transition state (TS) were optimized at the MP2 level using the energy-gradient technique. The TS was determined by calculating the Hessian matrix. In all of the calculations, the geometry of PH_3 was taken to be the same as the experimental structure of the free PH_3 molecule.[20] Then, MP2-MP4SDQ, SD-CI, and a coupled-cluster with double substitutions (CCD) calculations were carried out on those optimized geometries in order to evaluate the energy changes in the reaction. In all of these calculations, the core electrons were excluded from any active space. In the SD-CI calculation, the contribution of higher order excited configurations was estimated according to Davidson–Silver[21] and Pople et al.[22] In the CCD calculation, contributions from single and triple excitations were estimated with a perturbation based on the CCD wavefunction[23] (this method is described here as CCD (ST4)).

Four kinds of basis sets were used. In all of the basis sets, the core electrons of Rh (up to 3d) and Ir (up to 4f) were replaced with the effective core potentials (ECPs) of Hay and Wadt.[24] In the BS-I, (311/311/31) and (311/311/21) basis sets were used for the valence electrons of Rh and Ir, respectively.[24] MIDI-3 sets[25] were employed for C, O, Si, P, and Cl, and a (31) set was adopted for H.[26] A d-polarization function and a p-polarization function were added to Si[25b] and an active H atom[26] respectively, where the active H atom is the hydride ligand coordinating to the metal and the hydrogen atom changing into the hydride. The BS-I set was employed in the geometry optimization. In the BS-II, (311/311/211) and (311/311/111) basis sets were used for the valence electrons of Rh and Ir, respectively.[24] The MIDI-4 set was employed for C, O, P, Si, and Cl[25] along with the (31) set used for H.[26] In BS-III, a d-polarization function[25] was also added to C and O without any other modification of BS-II. In BS-IV, (531111/4211/1)[26,27] and (311)[28] were used for the Si and H atoms, respectively, without any other modification of BS-III. The p-polarization function was added to the active H atom, also in this set. The basis-set effects on the activation energy (E_a) and the reaction energy (ΔE) were examined using these BS-II—BS-IV. Finally, the BS-IV set was adopted for estimating the energy changes.

Results and Discussion

Geometry Changes. We considered that the reaction proceeds via the precursor complex (PC) and the transition state (TS) to yield the *cis*-silyl hydride complex. Because there are three possible reaction courses in this oxidative addition (Scheme 1), we examined all of the possible structures in PC, TS, and the product. Those optimized geometries are shown in Figs. 1 and 2. In *trans*-$[RhCl(CO)(PH_3)_2]$, the optimized Rh–Cl and Rh–P distances are slightly longer than those in similar *trans*-$[RhCl(CO)(PPh_3)_2]$ ($R(\text{Rh–Cl})=2.382$ Å and $R(\text{Rh–P})_{av}=2.322$ Å),[29] while the Rh–CO distance is somewhat longer than in $[RhCl(CO)(PPh_3)_2]$ ($R(\text{Rh–CO})=1.77$ Å). In *trans*-$[IrCl(CO)(PH_3)_2]$, the Ir–PH_3 and Ir–Cl distances are slightly longer than those in $[IrCl(CO)_2(PPh_3)_2]$ ($R(\text{Ir–P})=2.332$ Å and $R(\text{Ir–Cl})=2.37$ Å).[30] The calculated Ir–CO distance is somewhat shorter than in $[IrCl(CO)_2(PPh_3)_2]$ ($R(\text{Ir–CO})=2.04$ Å), probably because two CO molecules coordinate to Ir in the latter complex. It is believed that the calculated coordinate bond distance is improved by introducing a polarization function on the ligand atoms.[31—33] However, it was also ascertained that even if the geometry optimization was carried out with basis sets including no polarization function on the ligand atoms, the energy change might be reliably calculated on those optimized geometries with basis sets including a polarization function on the ligand atoms.[33] Moreover, the discrepancies between the optimized geometries and the experimental ones are small in this case. This means that although the bond distance optimized here would slightly deviate from that in the real geometry, the energy change presented here is considered to be reliable.

In all of the possible precursor complexes (PC), SiH_4 is distant from the metal complex, and both geometries of SiH_4 and $[MCl(CO)(PH_3)_2]$ distort only slightly from their equilibrium structures, like the precursor complex observed in the Si–H oxidative addition to $[M'(PH_3)_2]$.[2] Of three PCs, **PC3** is the most stable, whereas the energy difference between **PC3** and others is very small, being less than 1 kcal mol^{-1}.

In all TS structures,[34] the Si–H bond is lengthened to 1.65—1.5 Å for M=Ir and 1.64—1.78 Å for M=Rh. This is in contrast to the TS of the Si–H oxidative addition to $[M'(PH_3)_2]$ in which the Si–H bond is lengthened only slightly.[2] This difference is discussed below in relation to the activation energy (E_a) of the reaction.

Some knowledge concerning the *trans*-influence is deduced from the geometries of the products. Considering that the M–Cl distance becomes longer in the order **P3**<**P2**<**P1**, the *trans*-influence becomes stronger in the order CO<H<SiH_3. Our previous calculations of *cis*-$[M'H(SiH_3)(PH_3)_2]$ (M′=Pd or Pt) also indicated that SiH_3 has a stronger *trans*-influence than does H.[2] The M–CO distance becomes longer according to **P3**<**P1**<**P2**, indicating that the *trans*-influence increases in the order Cl<H<SiH_3. The M–SiH_3 distance becomes longer in the order **P1**<**P3**<**P2**, indicating that the *trans*-influence strengthens in the order Cl<PH_3<CO. The M–PH_3 distance also indicates that the *trans*-influence increases in the order PH_3<H<SiH_3, since this distance becomes longer in the order **P1**≈**P2**<**P3**, and M–PH_3 (*trans* to SiH_3) is longer than M–PH_3 (*trans* to H) (see **RhP3** and **IrP3** in Figs. 1 and 2). From the above results, it is reasonably concluded that the *trans*-influence increases in the order Cl<PH_3<CO<H<SiH_3.

Correlation Effects and Basis Set Effects. Prior to a detailed discussion, we mention here some correlation effects on the activation energy (E_a) and the reaction energy (ΔE). E_a is defined as the energy difference between TS and the most stable **PC3**, and ΔE is the energy difference between the product and reactants. As shown in Table 1, the introduction of correlation effects considerably decreases E_a and ΔE (i.e., increases the exothermicity E_{exo}) like in the C–H, Si–H, and

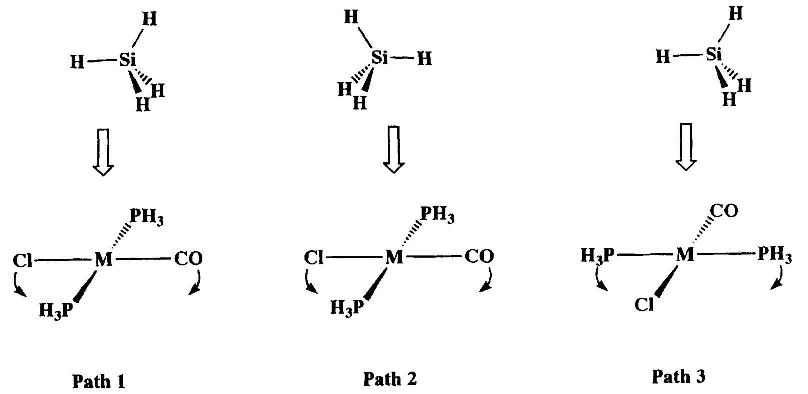

Scheme 1.

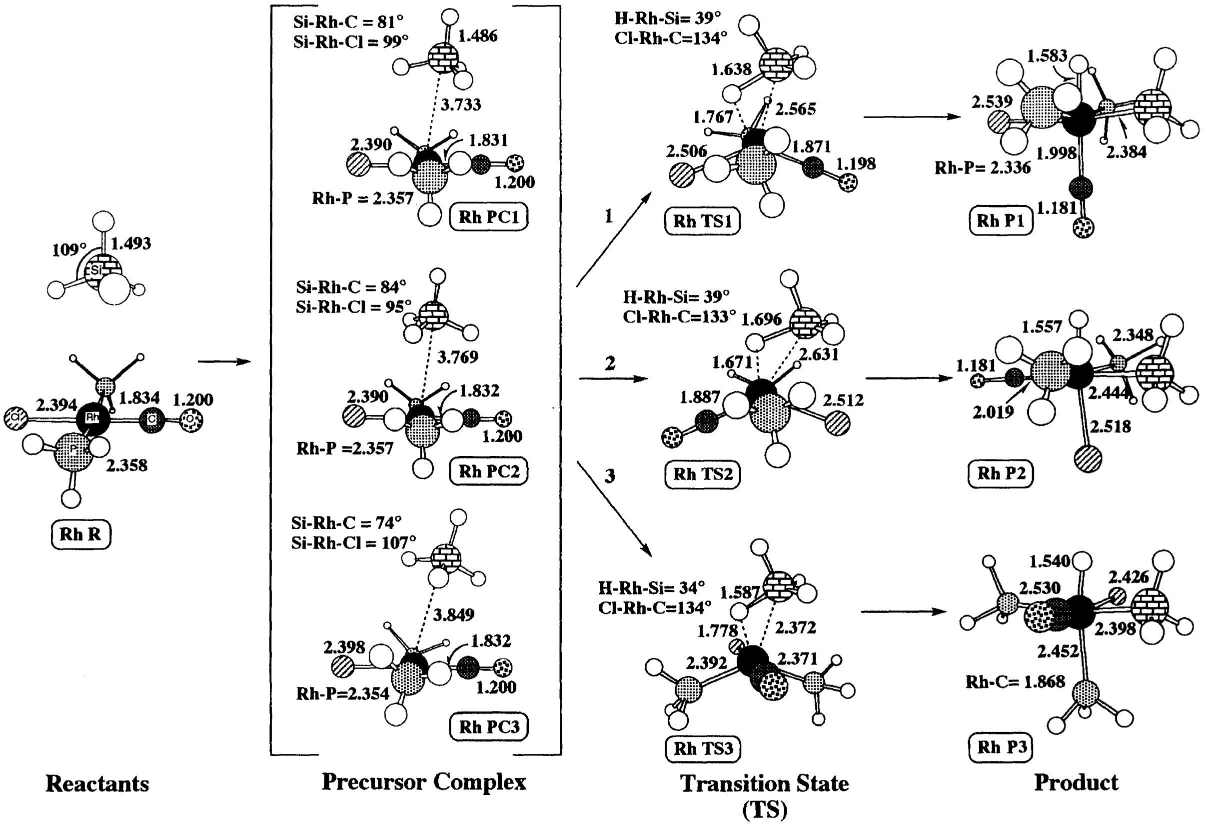

Fig. 1. Geometry changes in the Si–H oxidative addition to $RhCl(CO)(PH_3)_2$. Bond distances in Å and bond angles in degree.

Si–Si oxidative addition to $[M'(PH_3)_2]$[2] and $[RhCl(PH_3)_2]$.[3] In all of the TS, no instability of Hartree–Fock wavefunction was observed; the eigenvalue for the UHF instability is 0.030 for **RhTS1**, 0.022 for **RhTS2**, and 0.026 for **RhTS3**, 0.035 for **IrTS1**, 0.039 for **IrTS2**, and 0.037 for **IrTS3**, where the BS-II was used. This means that a single-reference wavefunction can be used to investigate this kind of oxidative addition. Previous papers[2d,35] also reported that a single reference wavefunction would be reliable in an oxidative addition to the second-row transition metal complexes. The E_a and ΔE values somewhat fluctuate upon going to MP4DQ from MP2, but fluctuate only little upon going to MP4SDQ from MP4DQ. The ΔE value is considerably different between the SD-CI and MP4SDQ levels, while the E_a value only slightly differs between the two methods. Furthermore, the CCD (ST4) method yields almost the same E_a and ΔE values as does the MP4SDQ method. In this work, therefore, the discussion is based on the MP4SDQ values.

Using the MP4SDQ method, the basis-set effects were investigated for the Rh system, as shown in Table 2. Upon going to BS-III from BS-II, the E_a value slightly increases and the reaction energy becomes somewhat less negative (i.e., less exothermic). Similar, but slightly smaller, changes further occur upon going to BS-IV from BS-III. From these results, we adopted BS-IV in estimating E_a and ΔE.

Relative Stabilities of Products. The previous experimental work indicated that the H–H oxidative addition to $[IrX(CO)(PR_3)_2]$ occurs in the X–Ir–CO plane to yield

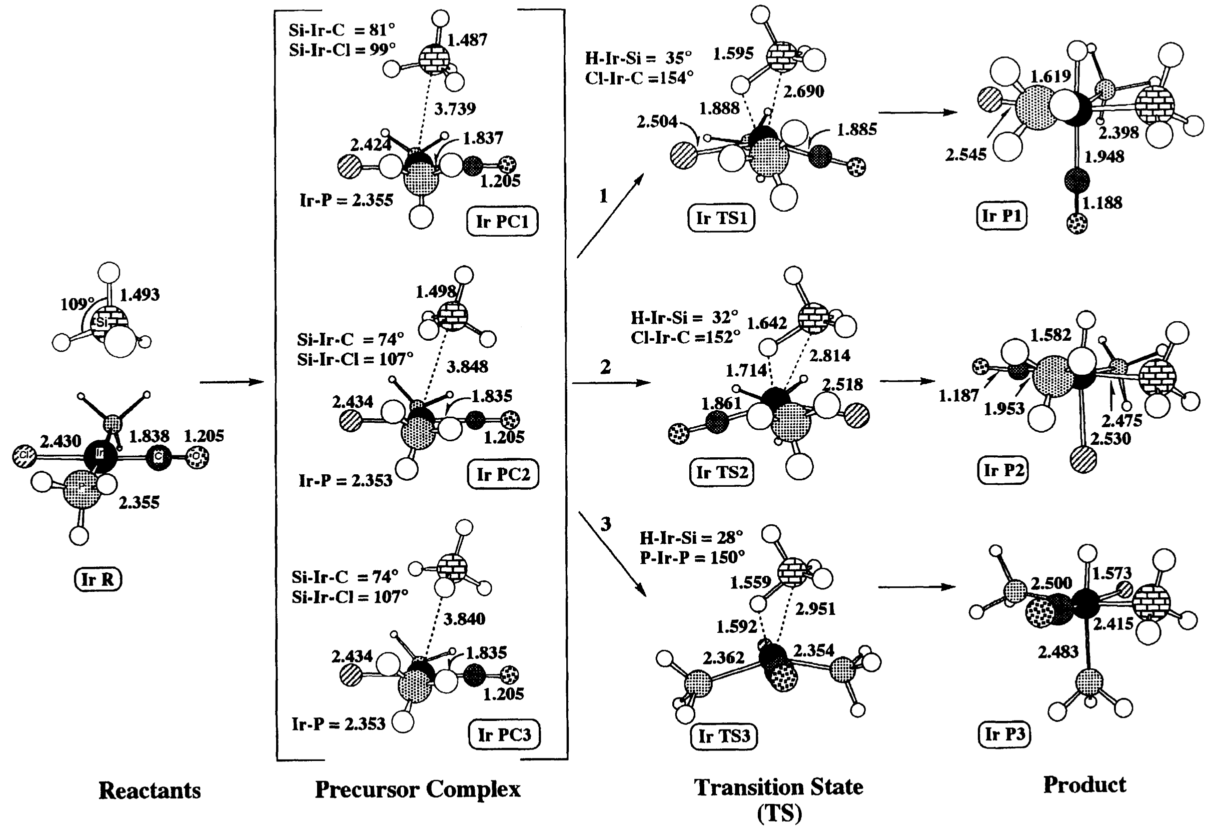

Fig. 2. Geometry changes in the Si–H oxidative addition to $IrCl(CO)(PH_3)_2$. Bond distances in Å and bond angles in degree.

Table 1. Correlation Effects on the Activation Energy (E_a) and the Reaction Energy (ΔE)[a] of the Si–H Oxidative Addition to $RhCl(CO)(PH_3)_2$

	E_a	ΔE
HF	23.8	20.6
MP2	9.7	−12.3
MP3	13.2	−3.5
MP4DQ	10.8	−9.6
MP4SDQ	10.2	−7.9
SD-CI(DS)[b]	11.8	−1.9
SD-CI(P)[c]	12.2	−1.4
CCD	12.4	−5.8
CCD (ST4)	11.0	−6.1

kcal mol^{-1}. BS-II was used. a) Reaction path 3. b) Davidson–Silver correction for higher order excited configurations (Ref. 21). c) Pople correction for higher order excited configurations (Ref. 22).

cis, *trans*-$[Ir(H)_2X(CO)(PR_3)_2]$ **1** (Scheme 2) when X=Cl or Br,[36] while the oxidative addition occurs in the P–Ir–P plane to yield *cis*, *cis*-$[Ir(H)_2X(CO)(PR_3)_2]$ **2** when X=H or CH_3.[36,37] According to an NMR investigation,[16] H is at a *trans*-position to SiH_3 in the product of the H–SiH_3 oxidative addition to $[IrCl(CO)(PR_3)_2]$ (see **3** in Scheme 2), while H is at a *cis*-position to GeH_3 in the product of a H–GeH_3 oxidative addition (**4** in Scheme 2). Although **3** is not considered to be a direct product from the Si–H oxidative addition, **4** is directly formed through the Ge–H oxidative addition which occurs in the Cl–Ir–(CO) plane, like the H–H oxidative addition. From these results, we examined two kinds of reaction courses (paths **1** and **2** in Scheme 1), leading to products **P1** and **P2**, as shown in Figs. 1 and 2.

However, recent theoretical calculations have indicated that the H–H oxidative addition to $[IrCl(CO)(PH_3)_2]$ occurs most easily on the PH_3–Ir–PH_3 plane,[11a] contrary to the experimental results.[36] Through a detailed inspection, it was clearly concluded that an oxidative addition to $[IrCl(CO)(PR_3)_2]$ occurs on the PH_3–Ir–PH_3 plane because PH_3 is weaker σ-donating and stronger π-accepting than PPh_3.[11a] Since PH_3 was adopted here as a model of PR_3, the Si–H ox-

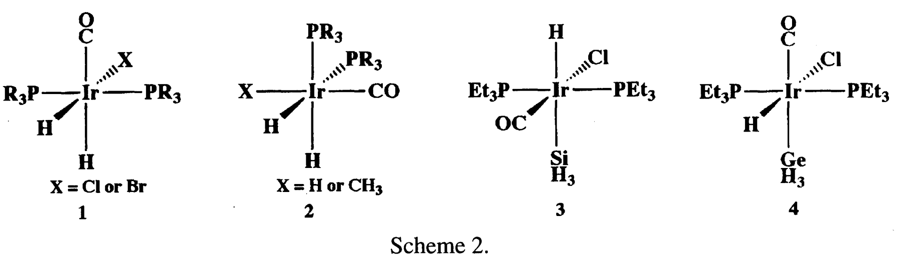

Scheme 2.

Table 2. The Binding Energy (BE),[a)] the Activation Energy (E_a),[b)] and the Reaction Energy (ΔE)[c)] of the Si–H Oxidative Addition to *trans*-MCl(CO)(PH$_3$)$_2$

Basis set[b)]	Path 1			Path 2			Path 3		
	BE	E_a	ΔE	BE	E_a	ΔE	BE	E_a	ΔE
M=Rh									
BS-II	−2.7	16.3	−6.1	−2.6	16.8	−3.5	−1.9	8.9	−7.9
BSIII	−2.9	17.9	−3.4	−2.8	18.6	−0.8	−2.2	9.6	−6.9
BS-IV	−2.4	18.7	−0.4	−2.3	19.4	0.3	−1.9	10.3	−5.5
M=Ir									
BS-IV		13.0	−17.4		13.1	−15.3		8.0	−22.3
Pd(PH$_3$)$_2$[d)]	−2.3	0.5	−6.6						
Pt(PH$_3$)$_2$[d)]	−2.2	2.4	−21.9						

MP4SDQ level. kcal mol^{-1}. a) The stabilization energy of the precursor complex (PCM) relative to reactants. b) E_a=E_t(TS)−E_t(PC3). c) ΔE=E_t(Product)−E_t(Reactants). d) Ref. 2d.

idative addition in the PH$_3$–Ir–PH$_3$ plane (path 3 in Scheme 1) was also investigated. This reaction course (path 3) is considered to be a model for a Si–H oxidative addition to [IrCl(CO)(PR$_3$)$_2$], when PR$_3$ is weak σ-donating, like phosphite.

As shown in Table 2, **P3** is the most stable among the three products; the next is **P1** and the least is **P3**, while **P1** is only slightly more stable than **P2**. These relative stabilities are consistent with the experimentally well-known *trans*-influence, i.e., Cl<PH$_3$<CO<H<SiH$_3$ (vide supra), as follows: In **P3**, two PH$_3$ ligands are at the *trans*-positions to H and SiH$_3$, which possess a strong *trans*-influence. This situation is the best because CO is at a *trans*-position neither to H nor to SiH$_3$. In **P1**, SiH$_3$ and H are at the *trans*-positions to Cl and CO, respectively. This situation is slightly better than in **P2** because **P2** has SiH$_3$ at a *trans*-position to CO, exhibiting a stronger *trans*-influence than Cl.

Here, we mention the stability of **3** (Scheme 2), since **3** was proposed based on an NMR investigation (vide supra).[16)] However, **3** was calculated to be much less stable than **IrP1** by 10.6 kcal mol^{-1} (MP4SDQ/BS-II). Thus, it is reasonably concluded that **3** is the least stable among all of the isomers of [IrCl(H)(SiH$_3$)(CO)(PH$_3$)$_2$]. This result is not surprising, since **3** has SiH$_3$ at a *trans*-position to H, and both SiH$_3$ and H exhibit a strong *trans*-influence. From these results, one should consider the possibility that [IrCl(H)(SiH$_3$)(CO)(PEt$_3$)$_2$] takes a structure like **IrP1**, and that a detailed reexamination of the NMR spectra will be necessary.[38)]

Activation Energy (E_a) and Reaction Energy (ΔE) of Three Reaction Courses. As shown in Table 2, the Si–H oxidative addition to [MCl(CO)(PH$_3$)$_2$] most easily proceeds via reaction path 3 with the lowest E_a value, to yield **P3**. As described above,[11a)] **P3** is considered to be the product of the Si–H oxidative addition when PR$_3$ is weak σ-donating. The other two reaction courses, paths 1 and 2, occur with a somewhat high E_a value of 19 kcal mol^{-1} for Rh and 13 kcal mol^{-1} for Ir. These reaction paths are a model of the oxidative addition when electron-donating phosphines coordinate to M. From these results, it is reasonably concluded that the weak σ-donating phosphine, such as phosphite and fluoroalkyl phosphine, favors the Si–H oxidative addition to a Vaska-type complex, which proceeds via path 3 to yield a **P3**-type product. Because a detailed discussion was presented concerning the reason that the H–H oxidative addition proceeds via path 3 with a lower E_a than those of paths 1 and 2 when PH$_3$ coordinates to M,[11a)] the discussion is not repeated here.

We now compare [IrCl(CO)(PH$_3$)$_2$] and [RhCl(CO)(PH$_3$)$_2$]. As clearly shown in Table 2, the Si–H oxidative addition to [IrCl(CO)(PH$_3$)$_2$] takes place with a much lower E_a and a much higher exothermicity (E_{exo}) than that to [RhCl(CO)(PH$_3$)$_2$] in all of the reaction paths. The difference in exothermicity is easily understood in terms of the bond energies. The M–H and M–SiH$_3$ bond energies are estimated through MP4SDQ/BS-IV calculations, considering the following equations:

$$[\mathrm{MCl(CO)(PH_3)_2}] + \mathrm{H_2} \longrightarrow [\mathrm{MCl(H)_2(CO)(PH_3)_2}], \tag{3}$$

$$[\mathrm{MCl(CO)(PH_3)_2}] + \mathrm{Si_2H_6} \longrightarrow [\mathrm{MCl(SiH_3)_2(CO)(PH_3)_2}], \tag{4}$$

$$[\mathrm{MCl(CO)(PH_3)_2}] + \mathrm{H{-}SiH_3} \longrightarrow [\mathrm{MCl(H)(SiH_3)(CO)(PH_3)_2}]. \tag{5}$$

As shown in Table 3, these bond energies somewhat fluctuate going from MP2 to MP3, but fluctuate only slightly upon going to MP4SDQ from MP4DQ. We discuss the exothermicity using the bond energy at the MP4SDQ level. The Ir–H and Ir–SiH$_3$ bond energies are much greater than the Rh–H and Rh–SiH$_3$ bond energies by ca. 10 and 6 kcal mol^{-1}, respectively. As a result, the oxidative addition to [IrCl(CO)(PH$_3$)$_2$] is more exothermic than that to [RhCl(CO)(PH$_3$)$_2$].

Here, it will be discussed why the Ir–H and Ir–SiH$_3$ bonds are stronger than the Rh–H and Rh–SiH$_3$ bonds. Since the M–H and M–SiH$_3$ bonds are considered to be covalent with some ionic character, we examine a metal fragment [MCl(CO)(PH$_3$)$_2$] which possesses two singly occupied orbitals, because the homolytic breaking of the M–H and M–SiH$_3$ bonds yields such a metal fragment. The energy levels of those singly occupied orbitals are calculated for the triplet state of [MCl(CO)(PH$_3$)$_2$] taking the same structure in **P1**. Apparently, the singly occupied d orbitals of Rh are at almost the same energy to those of Ir (Fig. 3). However, the d orbital

Table 3. M–H and M–Si–H Bond Energies[a)]

	Rh–H		Rh–SiH$_3$			Ir–H		Ir–SiH$_3$		
trans-Ligand[b)]	Cl, CO[c)]	PH$_3$	Cl	CO	PH$_3$	Cl, CO[c)]	PH$_3$	Cl	CO	PH$_3$
MP2	48.1	49.1	48.9	47.8	50.8	56.8	59.2	54.9	52.6	56.3
MP3	50.6	50.8	40.0	39.7	42.2	60.6	62.2	50.3	48.6	51.8
MP4DQ	51.0	52.8	45.5	44.8	46.8	59.8	61.9	52.4	50.4	54.1
MP4SDQ	48.2	50.0	44.4	43.5	47.6	58.0	60.7	51.5	49.5	53.8

	Pd–H[d)]	Pd–SiH$_3$[d)]	Pt–H[d)]	Pt–SiH$_3$[d)]
MP2	49.4	50.6	57.7	59.9
MP3	50.1	46.7	59.3	56.4
MP4DQ	51.5	48.0	59.1	57.1
MP4SDQ	52.1	48.8	58.7	57.6

a) BS-IV was used. b) The *trans*-positioned ligand to the M–X bond (M=Rh or Ir; X=H or SiH$_3$). c) The averaged value from M(H)$_2$Cl(CO)(PH$_3$)$_2$. d) Ref. 2.

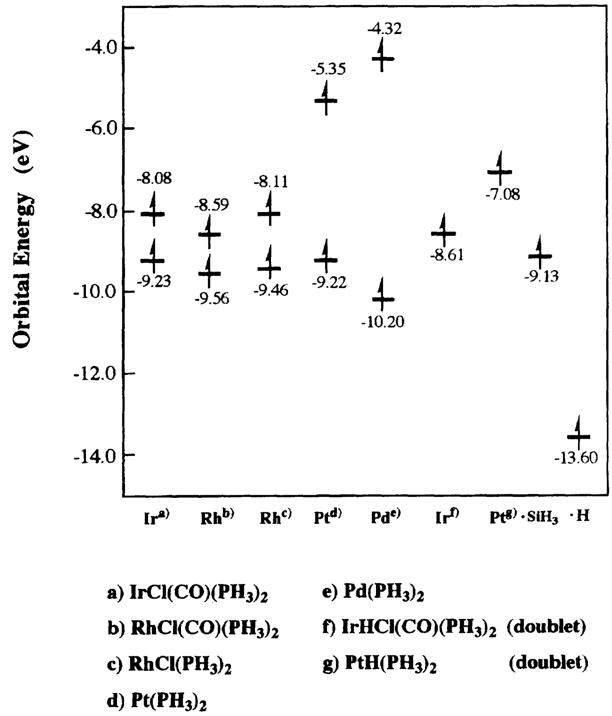

Fig. 3. Orbital energies of MCl(CO)(PH$_3$)$_2$, M(PH$_3$)$_2$, SiH$_3$, and H. The UHF/BS-IV calculations were carried out for triplet state of MCl(CO)(PH$_3$)$_2$ and M(PH$_3$)$_2$, and for doublet state for SiH$_3$ and H, where the geometry of metal fragment was taken to be the same as it in the product (**RhP1** and **IrP1**).

of the third-row transition metal generally expands more than that of the second-row transition metal (note that Rh–H and Rh–SiH$_3$ bond distances are similar to the Ir–H and Ir–SiH$_3$ bond distances, respectively, as shown in Figs. 1 and 2). Also, the 6p orbitals of Ir contribute more to the Ir–SiH$_3$ and Ir–H bonds than do the 5p orbitals of Rh, as shown by the electron population change: the Ir 6p orbital population increases by 1.287 e and the Rh 5p orbital population by 1.066 e in the Si–H oxidative addition (the path 1). This is because the Ir 6p orbital lies at a lower energy than the Rh 5p orbital.[39)] As a result, the Ir–SiH$_3$ and Ir–H bonds are stronger than the Rh–SiH$_3$ and Rh–H bonds. Thus, the Si–H oxidative addition to [IrCl(CO)(PH$_3$)$_2$] is more exothermic than it is to the Rh analogue.

A Comparison between RhCl(CO)(PH$_3$)$_2$ and RhCl(PH$_3$)$_2$. Previously, Koga and Morokuma theoretically investigated the Si–H oxidative addition to [RhCl(PH$_3$)$_2$].[3)] According to their calculations, this oxidative addition occurs with a zero barrier and a much high exothermicity (55 kcal mol^{-1} at MP4 level), to yield [RhClX(SiH$_3$)(PH$_3$)$_2$] (X=H or SiH$_3$), which takes a distorted trigonal bipyramid structure with an XRhSi angle of about 90° and two phosphines on the C_{3v} axis. Thus, there is a significant contrast between their results and ours, since the Si–H oxidative addition to [RhCl(CO)(PH$_3$)$_2$] requires a considerable E_a value and exhibits a small exothermicity (vide supra). This contrast is worthy of a detailed investigation. First, the exothermicity will be compared between two systems. The exothermicity is mainly determined by the Rh–H and Rh–SiH$_3$ bond energies. The Rh–SiH$_3$ bond energy of [RhCl(SiH$_3$)$_2$(PH$_3$)$_2$] was estimated to be about 78 kcal mol^{-1} at the MP2 level.[3)] This value is much larger than the Rh–SiH$_3$ bond energy in [RhCl(H)(SiH$_3$)(CO)(PH$_3$)$_2$], which was calculated to be 40—42 kcal mol^{-1} at the MP2 level and 44—47 kcal mol^{-1} at the MP4SDQ level (see Table 3). Thus, the Si–H oxidative addition to [RhCl(PH$_3$)$_2$] is more exothermic than that to [RhCl(CO)(PH$_3$)$_2$].

It is very interesting to investigate the reason that the Rh–H and Rh–SiH$_3$ bonds are stronger in [RhCl(H)(SiH$_3$)(PH$_3$)$_2$] than in [RhCl(H)(SiH$_3$)(CO)(PH$_3$)$_2$]. The d orbital energy is one of the important factors concerning the bond energy. Two singly occupied orbitals of the metal fragment are compared, as shown in Fig. 3. Although one d orbital of [RhCl(PH$_3$)$_2$] lies at a similar energy, the other is at a slightly higher energy than those of [RhCl(CO)(PH$_3$)$_2$]. These orbital energies seem not to give rise to a significant difference in the bond energy. The *trans*-influence is also considered to be an important factor for this difference. In the trigonal bipyramid structure of [RhCl(H)(SiH$_3$)(PH$_3$)$_2$], the Rh–H and Rh–SiH$_3$ bonds are at a *trans*-position to a nearly vacant site, which leads to very strong Rh–H and Rh–SiH$_3$ bonds. In [RhCl(H)(SiH$_3$)(CO)(PH$_3$)$_2$] **RhP1**, on the other hand, H and SiH$_3$

are at the *trans*-positions of CO and Cl because of a steric constraint of the six-coordinate complex. Since CO and Cl exhibit a much stronger *trans*-influence than does the vacant site, the Rh–H and Rh–SiH_3 bonds in **RhP1** are much weaker than in $[RhCl(H)(SiH_3)(PH_3)_2]$. Also, the Rh–H and Rh–SiH_3 bond formation by Eqs. 2, 3, 4, and 5 would weaken the Rh–Cl, Rh–CO, and Rh–PH_3 bonds, which is one of the plausible factors for determining the bond energy. For instance, **RhP1** and **RhP2** have much longer Rh–Cl and Rh–CO bonds, and **RhP3** has much longer Rh–PH_3 bonds than those of $[RhCl(CO)(PH_3)_2]$ (Fig. 1). This is not surprising because such strong ligands as H and SiH_3 are at the *trans*-position to Cl and CO in **P1** and **P2** and at the *trans*-position to PH_3 in **P3**. The bond weakening destabilizes the products, **P1**, **P2**, and **P3**, which leads to the small Rh–H and Rh–SiH_3 bond energies. On the other hand, although only a Rh–Cl bond is weakened, the Rh–PH_3 bond is somewhat strengthened by the Si–H oxidative addition to $[RhCl(PH_3)_2]$; R(Rh–Cl)=2.375 Å and R(Rh–P)=2.395 Å in $RhCl(PH_3)_2$, and R(Rh–Cl)=2.462 Å and R(Rh–P)=2.361 Å in $[RhH(SiH_3)Cl(PH_3)_2]$.[40] The other factors, such as a steric repulsion, more destabilize $[RhCl(H)_2(CO)(PH_3)_2]$, $[RhCl(SiH_3)_2(CO)(PH_3)_2]$, and $[RhCl(H)(SiH_3)(CO)(PH_3)_2]$ than $[RhClX(SiH_3)(PH_3)_2]$, because the former six-coordinate complexes are more crowded than the latter five-coordinate complex. From all of these factors, the formation of Rh–H and Rh–SiH_3 bonds yields less energy stabilization of **P1**, **P2**, and **P3** than that of $[RhCl(H)(SiH_3)(PH_3)_2]$; therefore, the Si–H oxidative addition to $[RhCl(CO)(PH_3)_2]$ is much less exothermic than to $[RhCl(PH_3)_2]$.

The situation at TS is also much different between $[RhCl(PH_3)_2]$ and $[RhCl(CO)(PH_3)_2]$. In the TS of the Ir and Rh reaction systems, the Si–H bond to be broken is not lengthened very much, but still exist. We thus investigate the bonding nature at the TS, considering the interaction between $[MCl(CO)(PH_3)_2]$ and SiH_4. There are three important interactions in the oxidative addition: one is the charge-transfer (CT) interaction from SiH_4 to $[MCl(CO)(PH_3)_2]$;[9,41] the second is the CT interaction from $[MCl(CO)(PH_3)_2]$ to SiH_4;[9,41] and the third is the exchange repulsion between SiH_4 and the occupied d_σ orbital.[2d] Thus, the occupied d_π and d_σ and the unoccupied sp orbitals play important roles in the oxidative addition. In the oxidative addition to $[RhCl(CO)(PH_3)_2]$, SiH_4 must approach Rh along the z-axis (see Scheme 1). Because Rh(I) has a doubly occupied d_{z^2} orbital in $[RhCl(CO)(PH_3)_2]$, the Si–H σ-bond causes an exchange repulsion with the Rh d_{z^2} orbital (Scheme 3), which disfavors an oxidative addition to $[RhCl(CO)(PH_3)_2]$. On the other hand, SiH_4 approaches Rh along the x-axis in the oxidative addition to $[RhCl(PH_3)_2]$. Since the Rh $d_{x^2-y^2}$ orbital is unoccupied in a formal sense, the approach of SiH_4 causes only a small exchange repulsion with $[RhCl(PH_3)_2]$. This unoccupied $d_{x^2-y^2}$ orbital also enhances the CT from the Si–H σ orbital to Rh in the oxidative addition to $[RhCl(PH_3)_2]$. The CT from the Rh d_π orbital to the Si–H σ^* orbital of SiH_4 depends on the Rh d_π orbital energy. As clearly shown in Fig. 4(a), the d_π orbital of $[RhCl(PH_3)_2]$ is at a higher energy than that of $[RhCl(CO)(PH_3)_2]$ by ca. 0.4 eV, probably because of the π-back bonding between Rh and CO in the latter complex. In other words, $[RhCl(CO)(PH_3)_2]$ should distort to push up the d_π orbital to a higher energy, which would cause some energy destabilization of $[RhCl(CO)(PH_3)_2]$, and would lead to a high E_a value. From all of these factors, the oxidative addition to $[RhCl(PH_3)_2]$ is much more favorable than to $[RhCl(CO)(PH_3)_2]$ from the viewpoints of both the activation energy and the reaction energy.

Comparison between Vaska-Type Complexes $[MCl(CO)(PH_3)_2]$ and $[M'(PH_3)_2]$ (M'=Pd or Pt). It is very interesting to compare Vaska-type complexes with $[M'(PH_3)_2]$. As clearly shown in Table 2, the Si–H oxidative addition to $[MCl(CO)(PH_3)_2]$ proceeds with a much higher E_a than that to $[M'(PH_3)_2]$, while the exothermicity is similar between $[IrCl(CO)(PH_3)_2]$ and $[Pt(PH_3)_2]$ and between $[RhCl(CO)(PH_3)_2]$ and $[Pd(PH_3)_2]$. Again, this similarity in the exothermicity is easily interpreted in terms of the bond energies. Interestingly, the Ir–H and Ir–SiH_3 bond energies are almost the same as the Pt–H and Pt–SiH_3 bond energies, respectively. Also, the Rh–H and Rh–SiH_3 bond energies are almost the same as the Pd–H and Pd–SiH_3 bond energies, respectively.

It would be interesting to understand the reason that the Ir–H and Ir–SiH_3 bonds are as strong as the Pt–H and Pt–SiH_3 bonds. First, the orbital energies are compared between $[Pt(PH_3)_2]$ and $[IrCl(CO)(PH_3)_2]$ which both take the geometries in the product.[42] As shown in Fig. 3, the d orbital of $[Pt(PH_3)_2]$ is at a similar energy to that of $[IrCl(CO)(PH_3)_2]$, while the sp orbital of $[Pt(PH_3)_2]$ is at a much higher energy than the d orbital of the Ir complex. If we consider the first bond-dissociation energy (Eqs. 6 and 7), the important factor

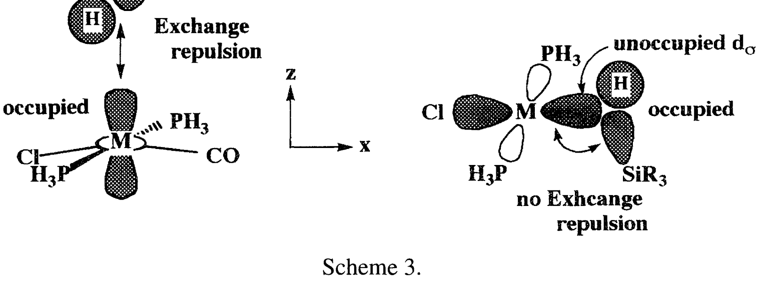

Scheme 3.

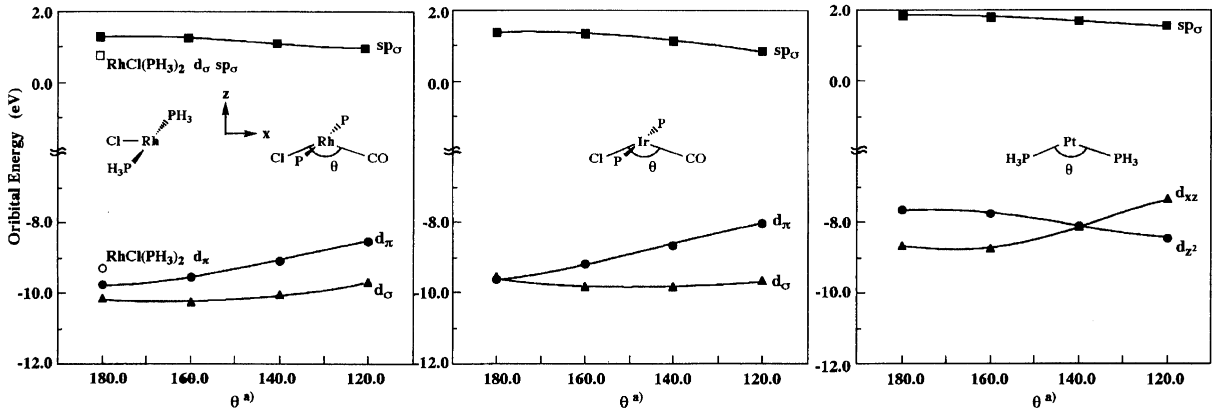

(a) **RhCl(CO)(PH$_3$)$_2$** (b) **IrCl(CO)(PH$_3$)$_2$** (c) **Pt(PH$_3$)$_2$**

Fig. 4. Energy levels of dσ, dπ, and spσ orbitals vs. distortion angle.

$$\textit{cis}\text{-}[\mathrm{M'(H)(SiH_3)(PH_3)_2}] \longrightarrow [\mathrm{M'(H)(PH_3)_2}] + \cdot\mathrm{SiH_3} \quad (6)$$

$$[\mathrm{MCl(H)(SiH_3)(CO)(PH_3)_2}] \longrightarrow [\mathrm{MCl(H)(CO)(PH_3)_2}] + \cdot\mathrm{SiH_3} \quad (7)$$

is the d$_\sigma$ orbital energy of the doublet [M$'$(H)(PH$_3$)$_2$] and [MCl(H)(CO)(PH$_3$)$_2$]. Again, the Ir d$_\sigma$ orbital energy (-8.6 eV) was calculated to be much more close to the radical orbital of $\cdot$SiH$_3$ than to the Pt d$_\sigma$ orbital (-7.1 eV), as shown in Fig. 3, while the first bond-dissociation energies of Ir–SiH$_3$ and Pt–SiH$_3$ were calculated to be similar (81.1 and 83.4 kcal mol^{-1} respectively at the MP4SDQ level). These results suggest that the Ir–H and Ir–SiH$_3$ bonds involve a much stronger covalent interaction than the Pt–H and Pt–SiH$_3$ bonds. Here, we must remember that although [RhCl(H)(SiH$_3$)$_2$(PH$_3$)$_2$] has much stronger Rh–H and Rh–SiH$_3$ bonds than does [RhCl(H)(SiH$_3$)(CO)(PH$_3$)$_2$], the d orbital energy is not responsible for this result. This result is interpreted in terms of a *trans*-influence, steric repulsion, and Rh–Cl and Rh–CO bond weakening. Of these three factors, the steric repulsion is also one of the plausible factors here. In [PtH(SiH$_3$)(PH$_3$)$_2$], SiH$_3$ and H receive a steric repulsion from two PH$_3$ ligands, while they receive a steric repulsion from three ligands in [MCl(H)(SiH$_3$)(CO)(PH$_3$)$_2$]; in **P1**, for instance, H receives a steric repulsion from two PH$_3$ and Cl, and SiH$_3$ receives it from two PH$_3$ and CO. The *trans*-influence should also be examined. SiH$_3$ is at a *trans*-position to PH$_3$ in [PtH(SiH$_3$)(PH$_3$)$_2$], at a *trans*-position to Cl in **IrP1**, at a *trans*-position to CO in **IrP2**, and at a *trans*-position to PH$_3$ in **IrP3**. However, the Ir–SiH$_3$ bond energy is similar in **IrP1**, **IrP2**, and **IrP3** (see Table 3), whereas the bond length considerably depends on the *trans*-positioned ligand. Thus, the *trans*-influence is not a main reason that the Pt–X bond (X=H or SiH$_3$) is as strong as the Ir–X bond in spite of the Pt sp orbital at a higher energy. The coordinate bond weakening of a co-existing ligand is also important for the energy change of Eqs. 2, 3, and 4. The Pt–PH$_3$ bond (2.314 Å in Pt(PH$_3$)$_2$) lengthens to 2.456 Å (averaged value) in *cis*-PtH(SiH$_3$)(PH$_3$)$_2$, while the Ir–PH$_3$ bond (2.355 Å in [IrCl(CO)(PH$_3$)$_2$]) lengthens to 2.492 Å (averaged value) in **IrP3**. The bond weakening seems to be similar in both the Pt and Ir reaction systems. From the above discussion, it is reasonably concluded that although the covalent interaction is stronger in the Ir–SiH$_3$ and Ir–H bonds than in the Pt–SiH$_3$ and Pt–H bonds, H and SiH$_3$ in *cis*-[PtH(SiH$_3$)(PH$_3$)$_2$] suffer a smaller steric repulsion than those in [IrCl(H)(SiH$_3$)(CO)(PH$_3$)$_2$]; as a result, the Pt–H and Pt–SiH$_3$ bonds are as strong as the Ir–H and Ir–SiH$_3$ bonds.

It is also worth clarifying the reason that although the Si–H oxidative addition to [MCl(CO)(PH$_3$)$_2$] is exothermic, similarly to the oxidative addition to [Pt(PH$_3$)$_2$], the former reaction requires a much higher E_a than the latter reaction. The d$_\pi$, d$_\sigma$, and sp$_\sigma$ orbital energies are given as a function of the distortion (see Fig. 4). Apparently, the d$_\pi$ orbital (HOMO) of [M$'$(PH$_3$)$_2$] is at a much higher energy than that of [MCl(CO)(PH$_3$)$_2$], even if the distortion is taken into consideration (the [Cl–Ir–CO)] angle is 154° for **IrTS1** and the P–Pt–P angle is 157° for the TS of Pt reaction system).[2b)] Thus, the CT interaction from [MCl(CO)(PH$_3$)$_2$] to SiH$_4$ is much weaker than that from [M$'$(PH$_3$)$_2$] to SiH$_4$. As a result, the Si–H bond should be more lengthened to effectively form this CT interaction in the oxidative addition to [MCl(CO)(PH$_3$)$_2$] than it is to [M$'$(PH$_3$)$_2$]. This means that the SiH$_4$ part is more destabilized in the TS, which disfavors the Si–H oxidative addition to [MCl(CO)(PH$_3$)$_2$]. The occupied d$_\sigma$ and unoccupied sp$_\sigma$ orbitals of [MCl(CO)(PH$_3$)$_2$] lie at lower energies than those in [M$'$(PH$_3$)$_2$], which yields a stronger CT interaction from SiH$_4$ to [MCl(CO)(PH$_3$)$_2$] and a smaller destabilization from the two-orbital four-electron repulsion between SiH$_4$ and [MCl(CO)(PH$_3$)$_2$] than in the oxidative addition to [Pt(PH$_3$)$_2$]. Thus, the higher E_a value in the oxidative addition to [MCl(CO)(PH$_3$)$_2$] is mainly attributed to the low-lying d$_\pi$ orbital.

Finally, we mention here the difference between [M$'$(PH$_3$)$_2$] and [RhCl(PH$_3$)$_2$]. The d$_\pi$ orbital of [M$'$(PH$_3$)$_2$] is at a higher energy than that of [RhCl(PH$_3$)$_2$]. Nevertheless, the Si–H oxidative addition to [RhCl(PH$_3$)$_2$] can occur with a zero barrier, as for [M$'$(PH$_3$)$_2$]. The *trans*-influence should be considered first: In [RhCl(H)(SiH$_3$)(PH$_3$)$_2$], H and SiH$_3$ suffer a small *trans*-influence (vide supra), while H and SiH$_3$

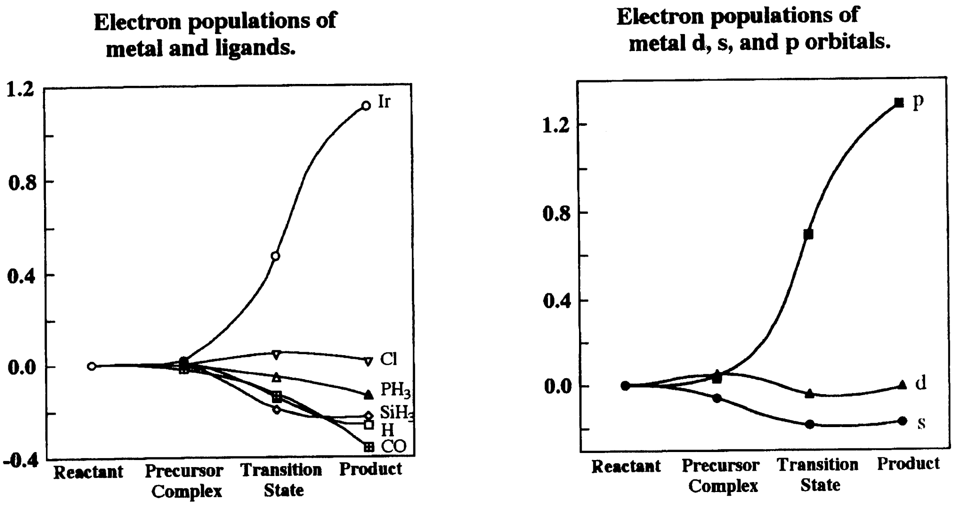

(a) $IrCl(CO)(PH_3)_2 + SiH_4 \longrightarrow Ir(H)(SiH_3)Cl(CO)(PH_3)_2$ (Path 1)

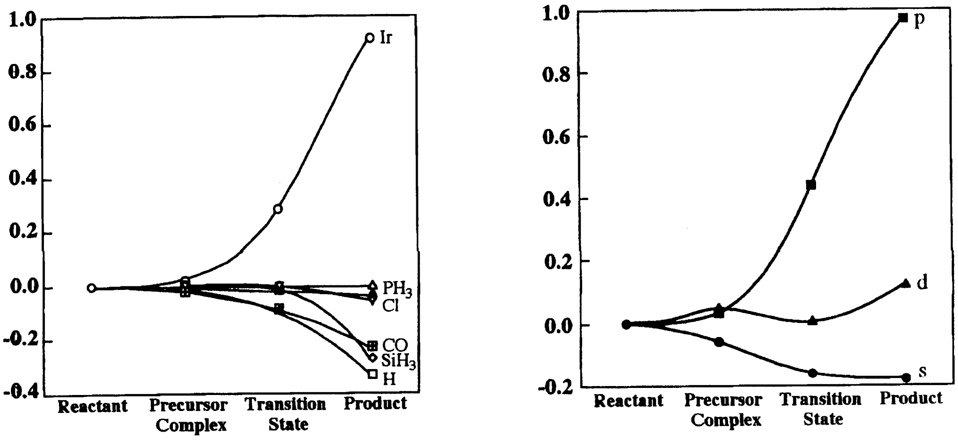

(b) $IrCl(CO)(PH_3)_2 + SiH_4 \longrightarrow Ir(H)(SiH_3)Cl(CO)(PH_3)_2$ (Path 3)

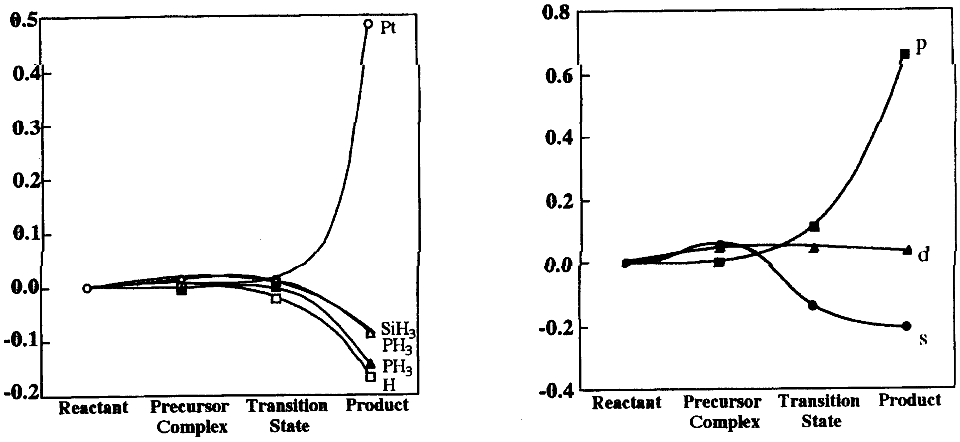

(c) $Pt(PH_3)_2 + SiH_4 \longrightarrow Pt(H)(SiH_3)(PH_3)_2$

Fig. 5. Electron distribution changes in the Si–H oxidative addition to $IrCl(CO)(PH_3)_2$ and $Pt(PH_3)_2$. The positive value represents an increase in Mulliken population and vice versa.

suffer a considerable *trans*-influence of PH_3 in *cis*-$[M'H(SiH_3)(PH_3)_2]$. The other is the energy level of the acceptor orbital of $[M'(PH_3)_2]$ and $[RhCl(PH_3)_2]$. In $[RhCl(PH_3)_2]$, the unoccupied $d_{x^2-y^2}$ orbital can form a CT interaction from SiH_4, while only a high-lying sp_σ orbital of $[M'(PH_3)_2]$ can participate in the CT interaction (Fig. 5). Also, the exchange repulsion between [RhCl(PH_3)$_2$] and SiH_4 is much less than that between [M′(PH_3)$_2$] and SiH_4, since the unoccupied $d_{x^2-y^2}$ orbital of [RhCl(PH_3)$_2$] does not cause such an exchange repulsion with SiH_4, but the occupied d_{z^2} orbital of [M′(PH_3)$_2$] causes it. Thus, the Si–H oxidative addition to [RhCl(PH_3)$_2$] easily proceeds like it to [M′(PH_3)$_2$],whereas the d orbital of [RhCl(PH_3)$_2$] is at a rather low energy.

Changes in Electron Distribution. The electron re-distribution is also interesting. As clearly shown in Fig. 5, several similarities are observed between the Ir and Pt systems (since similar results are observed in Rh and Pd systems, a discussion concerning them is omitted here for brevity). (1) The Ir atomic population increases in the product, which arises from a considerable increase in the Ir p orbital population (Figs. 5(a) and 5(b)). (2) The Ir s orbital population, on the other hand, decreases. (3) A similar electron re-distribution is observed in the Pt reaction system (Fig. 5(c)). These changes are interpreted in terms of a hybridization change caused in the reaction; the dsp^2 hybridization of square planar [IrCl(CO)(PH_3)$_2$] changes into the d^2sp^3 hybridization of octahedral-like [IrCl(H)(SiH_3)(CO)(PH_3)$_2$], while the sp hybridization of linear [Pt(PH_3)$_2$] changes into the dsp^2 hybridization of square planar [PtH(SiH_3)(PH_3)$_2$]. Both hybridization changes lead to an increase in the electron population of the metal p-orbital. The decrease in the s-orbital population would arise from the significant increase in the p-orbital contribution to the coordinate bond. (4) The electron populations of H and SiH_3 decrease in both the Ir and Pt systems, against our expectation based on the oxidative addition. (5) Consistent with these population changes of H and SiH_3, the d orbital populations of Ir and Pt decrease little. (6) The electron population of PH_3 considerably decreases in the Pt system, while that of CO significantly decreases, but that of PH_3 little changes in the Ir system. This can be attributed to the stronger donating ability of CO than that of PH_3; because the charge-transfer (CT) from CO is greatly enhanced in the product, the CT from PH_3 does not need to increase very much in the Ir reaction system.

In conclusion, the electron re-distribution caused by the Si–H oxidative addition to [MCl(CO)(PH_3)$_2$] is similar to it in the oxidative addition to [M′(PH_3)$_2$]. The main features of the electron re-distribution arise from the hybridization change.

Concluding Remarks

The Si–H oxidative addition to Vaska-type complexes, [MCl(CO)(PH_3)$_2$] (M=Rh or Ir), was theoretically investigated with ab initio MO/MP2—MP4, SD-CI, and CCD methods, where all of the geometries were optimized using the energy-gradient technique at the MP2 level. The introduction of electron correlation effects is indispensable for correctly estimating the E_a and E_{exo} values of this Si–H oxidative addition, as expected. The MP4DQ, MP4SDQ, CCD, and CCD(ST4) methods provide similar E_a and E_{exo} values, while the MP2 and MP3 methods yield somewhat different E_a and E_{exo} values, and the SD-CI method yields considerably small E_{exo} values. The Si–H oxidative addition to [IrCl(CO)(PH_3)$_2$] occurs with a smaller E_a and a larger E_{exo} than to [RhCl(CO)(PH_3)$_2$], which is interpreted in terms that the Ir–H and Ir–SiH_3 bonds are stronger than the Rh–H and Rh–SiH_3 bonds respectively. The oxidative addition to Vaska-type complexes exhibits some similarities to and some differences form [M′(PH_3)$_2$]: the exothermicity is similar in both reaction systems, while the Si–H oxidative addition to Vaska-type complexes requires a higher E_a than to [M′(PH_3)$_2$]. The lower reactivity of Vaska-type complexes arises from the d_π orbital at a low energy and the greater steric repulsion in the product. The electron re-distribution is similar in both systems, which is interpreted in terms of a hybridization change. The reactivity of the Vaska-type complex is very different from that of [RhCl(PH_3)$_2$]. The lower reactivity of [RhCl(CO)(PH_3)$_2$] is explained in terms of the greater weakening of Rh–Cl and Rh–CO bonds, the larger steric repulsion in the octahedral geometry, and the greater exchange repulsion between SiH_4 and the Rh d_{z^2} orbital. From the above discussion, it is reasonably predicted that the CO coordination to metal greatly disfavors oxidative additions.

This work was in part supported by a Grant-in-Aid for Scientific Research on Priority Area of Reactive Organometallics Nos. 07216258 and 04243102 from the Ministry of Education, Science and Culture. All of the computations were carried out with IBM RS-6000/360 and 3AT workstations in our laboratory and an sp^2 workstation of the Institute for Molecular Science (Okazaki, Japan).

References

1) For instance: a) I. Ojima, in "The Chemistry of Organic Silicon Compounds," ed by S. Patai and Z. Rappoport, John Wiley & Sons Ltd., New York (1989), p. 1479 ; b) T. D. Tilley, in "The Chemistry of Organic Silicon Compounds," ed by S. Patai and Z. Rappoport, John Wiley & Sons Ltd., New York (1989), p. 1415.

2) a) S. Sakaki and M. Ieki, *J. Am. Chem. Soc.*, **113**, 5063 (1991); b) S. Sakaki and M. Ieki, *J. Am. Chem. Soc.*, **115**, 2372 (1993); c) S. Sakaki, M. Ogawa, Y. Musashi, and T. Arai, *Inorg. Chem.*, **33**, 1660 (1994); d) S. Sakaki, M. Ogawa, and M. Kinoshita, *J. Phys. Chem.*, **99**, 9933 (1995).

3) K. Koga and K. Morokuma, *J. Am. Chem. Soc.*, **115**, 6883 (1993).

4) a) A. Dedieu and A. Strich, *Inorg. Chem.*, **18**, 2940 (1979); b) A. Dedieu, *Inorg. Chem.*, **19**, 375 (1980).

5) a) K. Kitaura, S. Obara, and K. Morokuma, *J. Am. Chem. Soc.*, **103**, 2891 (1981); b) S. Obara, K. Kitaura, and K. Morokuma, *J. Am. Chem. Soc.*, **106**, 7482 (1984).

6) a) J. O. Noell and P. J. Hay, *J. Am. Chem. Soc.*, **104**, 4578 (1982); b) P. J. Hay, *Chem. Phys. Lett.*, **103**, 466 (1984); c) P. J. Hay, *J. Am. Chem. Soc.*, **109**, 705 (1987).

7) a) M. R. A. Blomberg and P. E. M. Siegbahn, *J. Chem. Phys.*, **78**, 986 and 5682 (1983); b) M. R. A. Blomberg, U. Brandemark, L. Pettersson, and P. E. M. Siegbahn, *Int. J. Quantum Chem.*, **23**, 855 (1983); c) P. E. M. Siegbahn, M. R. A. Blomberg, and M. Svensson, *J. Am. Chem. Soc.*, **115**, 4191 (1993).

8) a) J. J. Low and W. A. Goddard, *J. Am. Chem. Soc.*, **106**, 6928 (1984); b) J. J. Low and W. A. Goddard, *Organometallics*, **5**,

609 (1986).

9) J. Y. Saillard and R. Hoffmann, *J. Am. Chem. Soc.*, **106**, 2006 (1984).

10) a) E. Folga, T. Ziegler, and L. Fan, *New J. Chem.*, **15**, 741 (1991); b) E. Folga and T. Ziegler, *Can. J. Chem.*, **70**, 333 (1992); c) T. Ziegler, E. Folga, and A. Berces, *J. Am. Chem. Soc.*, **115**, 636 (1993); d) J. Li, R. M. Dickson, and T. Ziegler, *J. Am. Chem. Soc.*, **117**, 11482 (1995).

11) a) A. L. Sargent and M. B. Hall, *Inorg. Chem.*, **31**, 317 (1992); b) A. L. Sargent, M. B. Hall, and M. F. Guest, *J. Am. Chem. Soc.*, **114**, 517 (1992).

12) J. J. Low and W. A. Goddard, *J. Am. Chem. Soc.*, **108**, 6115 (1986).

13) a) M. R. A. Blomberg, P. E. M. Siegbahn, U. Nagashima, and T. Wennerberg, *J. Am. Chem. Soc.*, **113**, 424 (1991); b) M. Svensson, M. R. A. Blomberg, and P. E. M. Siegbahn, *J. Am. Chem. Soc.*, **113**, 7076 (1991); c) M. R. A. Blomberg, P. E. M. Siegbahn, and M. Svensson, *J. Am. Chem. Soc.*, **114**, 6095 (1992); d) P. E. M. Siegbahn, M. R. A. Blomberg, and M. Svensson, *J. Am. Chem. Soc.*, **115**, 1952 (1993); e) P. E. M. Siegbahn, M. R. A. Blomberg, and M. Svensson, *J. Am. Chem. Soc.*, **115**, 4191 (1993); f) M. R. A. Blomberg, P. E. M. Siegbahn, and M. Svensson, *J. Phys. Chem.*, **98**, 2062 (1994); g) P. E. M. Siegbahn, *Organometallics*, **13**, 2833 (1994).

14) T. Ziegler, V. Tschinke, L. Fan, and A. D. Becke, *J. Am. Chem. Soc.*, **111**, 9177 (1989).

15) P. E. M. Siegbahn and M. R. A. Blomberg, *J. Am. Chem. Soc.*, **114**, 10548 (1992).

16) E. A. V. Ebsworth and T. E. Fraser, *J. Chem. Soc., Dalton Trans.*, **1979**, 1960.

17) C. E. Johnson and R. Eisenberg, *J. Am. Chem. Soc.*, **107**, 3148 and 6531 (1985).

18) M. A. Esteruelas, F. J. Lahoz, M. Oliován, E. Oñate, and L. A. Oro, *Organometallics*, **13**, 4246 (1994).

19) B. P. Cleary, R. Mehta, and R. Eisenberg, *Organometallics*, **14**, 2297 (1995).

20) G. Herzverg, "Molecular Spectra and Molecular Structure," Academic Press, New York (1974), Vol. 3, p. 267.

21) E. R. Davidson and D. W. Silver, *Chem. Phys. Lett.*, **52**, 403 (1977).

22) J. A. Pople, R. Seeger, and R. Krishnan, *Int. J. Quantum Chem., Symp.*, **11**, 149 (1977).

23) K. Raghavachari, *J. Chem. Phys.*, **82**, 4607 (1985).

24) P. J. Hay and W. R. Wadt, *J. Chem. Phys.*, **82**, 299 (1985).

25) a) S. Huzinaga, J. Andzelm, M. Klobukowski, E. Radio-Andzelm, Y. Sakai, and H. Tatewaki, "Gaussian Basis Sets for Molecular Calculations," Elsevier, Amsterdam (1984); b) Y. Sakai, H. Tatewaki, and S. Huzinaga, *J. Comput. Chem.*, **2**, 108 (1981).

26) T. H. Dunning and P. J. Hay, in "Methods of Electronic Structure Theory," ed by H. F. Schaeffer, Plenum, New York (1977), p. 1.

27) ζ_d=0.50, taken from the works by Schaefer and co-workers; for instance: G. Vacek, B. T. Colegrove, and H. F. Schaefer, *J. Am. Chem. Soc.*, **113**, 3192 (1991); R. S. Grev, H. F. Schaefer, and K. M. Baines, *J. Am. Chem. Soc.*, **112**, 9458 (1990).

28) T. H. Dunning, *J. Chem. Phys.*, **55**, 716 (1971).

29) K. R. Dunbar and S. C. Haefner, *Inorg. Chem.*, **31**, 3676 (1992).

30) N. C. Pavne and J. A. Ibers, *Inorg. Chem.*, **8**, 2715 (1969).

31) K. E. Frankcombe, K. J. Cavell, B. F. Yates, and R. B. Knott, *J. Phys. Chem.*, **99**, 14316 (1995).

32) G. Pacchioni and P. S. Bagus, *Inorg. Chem.*, **31**, 4391 (1992).

33) S. Sakaki, H. Satoh, H. Shono, and Y. Ujino, *Organometallics*, **15**, 1713 (1996).

34) The geometry of TS is intermediate between the reactant and the product. Moreover, one eigenvector with a negative eigenvalue was obtained from diagonalization of the Hessian matrix, and it involves the M–Si, M–H, and Si–H bond distances as its large components. Thus, although the IRC calculation was not carried out due to the large size of reaction system, the geometry of TS seems to be on the way connecting the reactant and the product.

35) P. E. M. Siegbahn and M. Svensson, *Chem. Phys. Lett.*, **216**, 147 (1993).

36) M. J. Burk, M. P. McGraph, R. Wheeler, and R. H. Crabtree, *J. Am. Chem. Soc.*, **110**, 5034 (1988), and references are therein.

37) J. F. Harrod and W. J. Yorke, *Inorg. Chem.*, **20**, 1156 (1981).

38) If PEt_3 is adopted in the calculation instead of PH_3, this energy difference would not be changed very much, since two PH_3 are at a trans to each other in both **3** and **IrP1**.

39) a) The Ir 6p orbital is calculated to be at a lower energy by 0.45 eV than the Rh 5p orbital in a model system $MH(PH_3)_2$ (M=Rh or Ir), where its $d_\sigma \rightarrow p_\pi$ triplet state was calculated with the UHF/BS-II method: *R*(M–H) and *R*(M–P) were rather arbitrarily taken to be 1.6 and 2.3 Å respectively; b) The Ir 6s and Rh 5s orbitals seem not to contribute very much to the fact that Ir–H and $Ir–SiH_3$ bonds are stronger than Rh–H and $Rh–SiH_3$ bonds. This is consistent with their population changes (see discussion on the electron redistribution). The reason is still ambiguous and further investigation on the role of s orbital is necessary.

40) N. Koga, private communication.

41) K. Tatsumi, R. Hoffmann, A. Yamamoto, and J. K. Stille, *Bull. Chem. Soc. Jpn.*, **54**, 1857 (1981).

42) Important are tow radical orbitals in the triplet state of $M(PH_3)_2$ and $MCl(CO)(PH_3)_2$, when we consider the sum of M–H and $M–SiH_3$ bond energies.